Articles

Synthesis, Characterization, and X-ray Structure of the Zirconium Bis(porphyrinate) Di(π-radical-cation) Complex $[Zr(TPP)_2][SbCl_6]_2$ and X-ray Structure of the Mono(π-radical-cation) Complex $[Zr(TPP)_2][SbCl_6]$

Hee-Joon Kim, Dongmok Whang, Jaheon Kim, and Kimoon Kim*

Department of Chemistry and Center for Biofunctional Molecules, Pohang Institute of Science and Technology, P.O. Box 125 Pohang 790-600, South Korea

Received December 4, 1991

The di(π-radical-cation) complex $[Zr(TPP)_2][SbCl_6]_2$ (TPP = *meso*-tetraphenylporphyrin dianion) was synthesized and fully characterized. Spectroscopic and magnetic susceptibility data of the dication complex indicate a strong antiferromagnetic coupling between the unpaired electrons residing on the two porphyrin rings. One notable feature of the dication complex is the high-energy near-IR absorption band which appears at 780 nm in the visible region. X-ray structures of $[Zr(TPP)_2][SbCl_6]$ and $[Zr(TPP)_2][SbCl_6]_2$ reveal that the interporphyrin distances shorten progressively as one proceeds from the neutral to the dication species. These structural features are consistent with the spectroscopic data and confirm that the $\pi\pi$ interaction between the two porphyrin rings is enhanced by oxidation. Crystallographic data for $[Zr(TPP)_2][SbCl_6]\cdot 3CH_2Cl_2$ (**2**): tetragonal, $P4/ncc$, $a = 21.260$ (3) Å, $c = 18.042$ (5) Å, $V = 8155$ (2) Å^3, $Z = 4$, $d_{calc} = 1.551$ g cm^{-3}, $T = 23$ °C, $R = 0.054$ and $R_w = 0.063$ for 1333 absorption-corrected reflections with $I > 3\sigma(I)$. $[Zr(TPP)_2][SbCl_6]_2\cdot 3CH_2Cl_2$ (**3**): monoclinic, $P2_1/c$, $a = 18.555$ (3) Å, $b = 18.037$ (2) Å, $c = 27.468$ (5) Å, $\beta = 102.95$ (2)°, $V = 8959$ (2) Å^3, $Z = 4$, $d_{calc} = 1.661$ g cm^{-3}, $T = -100$ °C, $R = 0.079$ and $R_w = 0.090$ for 3196 absorption-corrected reflections with $I > 3\sigma(I)$.

Introduction

Sandwich-type metal bis(tetrapyrrole) complexes have received considerable attention. For instance, rare earth metal bis(phthalocyanine) complexes[1] were studied intensively because of their electrical conductivity and electrochromic properties; the corresponding bis(porphyrin) complexes[2-5] have been studied as structural and spectroscopic models of the special pair in the reaction center[6] of photosynthesis. Until recently, such sandwich complexes have only been prepared with metal ions that possess very large ionic radii (>1 Å) such as yttrium,[2f] the lanthanides,[2] and the actinides.[3] We[7a] and others[7b] recently reported the synthesis and X-ray structure of the transition metal bis(porphyrin) complex $Zr(TPP)_2$ (**1**),[8] in which the two porphyrin rings are held in unusually close proximity due to the smaller ionic radius of Zr^{4+} (ca. 0.84 Å).[9] This compound and its monocation complex $[Zr(TPP)_2][SbCl_6]$ (**2**) exhibit interesting and unusual properties[7,10] as a result of the short distance between the two porphyrin rings. Here we report the synthesis and characterization of the dication complex $[Zr(TPP)_2][SbCl_6]_2$ (**3**)[11] and X-ray structures of the π-radical-cation complexes **2** and **3**, which reveal even shorter interplanar distances between the porphyrin rings.

Experimental Section

All chemicals were of reagent grade and were used without further purification except as noted below. All manipulations were performed with Schlenkware and cannula techniques under an argon atmosphere. Argon was purified by passage through successive columns of activated

(1) (a) Kirin, I. S.; Moskalev, P. N. *Russ. J. Phys. Chem.* (*Engl. Transl.*) **1967**, *41*, 251. (b) Moskalev, P. N.; Kirin, I. S. *Russ. J. Phys. Chem.* (*Engl. Transl.*) **1972**, *46*, 1019-1022. (c) Walton, D.; Ely, B.; Elliot, G. *J. Electrochem. Soc.* **1981**, *128*, 2479-2484. (d) Andre, J. J.; Simon, J.; Even, R.; Boudjema, B.; Guillaud, G.; Maitrot, M. *Synth. Met.* **1987**, *18*, 683-688. (e) Tomilova, L. G.; Ovchinnikiva, N. A.; Luk'yanets, E. A. *Zh. Obshch. Khim.* **1987**, *57*, 2100-2103. (f) Silver, J.; Lukes, P. J.; Key, P. K.; O'Connor, J. M. *Polyhedron* **1989**, *8*, 1631-1635. (g) Ercolani, C.; Paoletti, A. M.; Pennesi, G.; Rossi, G.; Chiesi-Villa, A.; Rizzoli, C. *J. Chem. Soc., Dalton Trans.* **1990**, 1971-1977.

(2) (a) Buchler, J. W.; Kapellmann, H.-G.; Knoff, M.; Lay, K.-L.; Pfeifer, S. *Z. Naturforsch.* **1983**, *38B*, 1339-1345. (b) Buchler, J. W.; De Cian, A.; Fischer, J.; Kihn-Botulinski, M.; Paulus, H.; Wiess, R. *J. Am. Chem. Soc.* **1986**, *108*, 3652-3659. (c) Buchler, J. W.; Elasser, K.; Kihn-Botulinski, M.; Scharbert, B. *Angew. Chem., Int. Ed. Engl.* **1986**, *25*, 286-287. (d) Buchler, J. W.; Scharbert, B. *J. Am. Chem. Soc.* **1988**, *110*, 4272-4276. (e) Buchler, J. W.; De Cian, A.; Fischer, J.; Kihn-Botulinski, M.; Wiess, R. *Inorg. Chem.* **1988**, *27*, 339-345. (f) Buchler, J. W.; Huttermann, J.; Loffler, J. *Bull. Chem. Soc. Jpn.* **1988**, *61*, 71-77. (g) Buchler, J. W.; De Cian, A.; Fisher, J.; Hammerschmitt, P.; Loffler, J.; Scharbert, B.; Weiss, R. *Chem. Ber.* **1989**, *122*, 2219-2228. (h) Buchler, J. W.; Hammerschmitt, P.; Kaufeld, I.; Loffler, J. *Chem. Ber.* **1991**, *124*, 2151-2159.

(3) (a) Girolami, G. S.; Milam, S. N.; Suslick, K. S. *Inorg. Chem.* **1987**, *26*, 343-344. (b) Girolami, G. S.; Milam, S. N.; Suslick, K. S. *J. Am. Chem. Soc.* **1988**, *110*, 2011-2012.

(4) (a) Yan, X.; Holten, D. *J. Phys. Chem.* **1988**, *92*, 409-414. (b) Bilsel, O.; Rodriguez, J.; Holten, D. *J. Phys. Chem.* **1990**, *94*, 3508-3512. (c) Bilsel, O.; Rodriguez, J.; Holten, D.; Girolami, G. S.; Milam, S. N.; Suslick, K. S. *J. Am. Chem. Soc.* **1990**, *112*, 4075-4077.

(5) (a) Donohoe, R. J.; Duchowski, J. K.; Bocian, D. F. *J. Am. Chem. Soc.* **1988**, *110*, 6119-6124. (b) Duchowski, J. K.; Bocian, D. F. *J. Am. Chem. Soc.* **1990**, *112*, 3312-3318. (c) Duchowski, J. K.; Bocian, D. F. *J. Am. Chem. Soc.* **1990**, *112*, 8807-8811. (d) Duchowski, J. K.; Bocian, D. F. *Inorg. Chem.* **1990**, *29*, 4158-4160. (e) Perng, J.-H.; Duchowski, J. K.; Bocian, D. F. *J. Phys. Chem.* **1990**, *94*, 6684-6691. (f) Perng, J.-H.; Duchowski, J. K.; Bocian, D. F. *J. Phys. Chem.* **1991**, *95*, 1319-1323.

(6) For a review: Deisenhofer, J.; Michel, H. *Science* **1989**, *245*, 1463-1473.

(7) (a) Kim, K.; Lee, W. S.; Kim, H.-J.; Cho, S.-H.; Girolami, G. S.; Gorlin, P. A.; Suslick, K. S. *Inorg. Chem.* **1991**, *30*, 2652-2656. (b) Buchler, J. W.; De Cian, A.; Fischer, J.; Hammerschmitt, D.; Wiess, R. *Chem. Ber.* **1991**, *124*, 1051-1058.

(8) TPP = 5,10,15,20-tetraphenylporphyrin dianion.

(9) Shannon, R. D. *Acta Crystallogr.* **1976**, *A32*, 751-767.

(10) (a) Bilsel, O.; Buchler, J. W.; Hammerschmitt, P.; Rodriguez, J.; Holten, D. *Chem. Phys. Lett.* **1991**, *182*, 415-421. (b) Lee, M.; Song, O.-K.; Seo, J.-C.; Kim, D.; Kim, H.-J.; Kim, K. *J. Phys. Chem.*, in press.

(11) Buchler and co-workers have reported[7b] the generation of the dication $Zr(TPP)^{2+}$ by electrochemical methods and its near-IR absorption spectrum.

0020-1669/92/1331-3882$03.00/0

molecular sieves 13X (Aldrich) and Ridox (Fisher). $H_2(TPP)$[12] and phenoxathiinylium hexachloroantimonate[13] were prepared by literature methods. $Zr(TPP)_2$ and $[Zr(TPP)_2][SbCl_6]$ were prepared by our previously reported procedures.[7a] CH_2Cl_2 and toluene were distilled from P_2O_5 and sodium benzophenone ketyl solution under a nitrogen atmosphere, respectively. UV–visible and near-IR spectra were recorded on a Hewlett-Packard 8542A or a Perkin-Elmer Lamda 15 spectrophotometer. ^1H NMR spectra were obtained from a Bruker AM 300 spectrometer. FT-infrared spectra were obtained on a Bomem DA3.01. EPR spectra were recorded in frozen CH_2Cl_2 at 100 K on a Bruker ER 200D-SRC spectrometer.

Synthesis of Bis(5,10,15,20-tetraphenylporphyrinato)zirconium(IV) Bis(hexachloroantimonate), $[Zr(TPP)_2][SbCl_6]_2$ (3). $Zr(TPP)_2$ (50 mg, 38 μmol) and phenoxathiinylium hexachloroantimonate (43 mg, 80 μmol) were placed in a 50-mL Schlenk flask. Dried CH_2Cl_2 (ca. 15 mL) was added to the flask with a cannula, and the solution was stirred for 2 h under purified Ar. During this time, a color change from orange-red to red-brown was observed and the reaction was monitored by UV–vis spectroscopy. After completion of the reaction, the solvent was removed in vacuo. Recrystallization from CH_2Cl_2/toluene under Ar yielded 66 mg of $[Zr(TPP)_2][SbCl_6]_2$ (88%). UV–vis, near-IR (CH_2Cl_2, nm): λ_{max} (log ε) 372 (4.88), 433 (sh), 505 (3.96), 780 (3.82, fwhm = 130 nm). ^1H NMR (CD_2Cl_2, –40 °C): δ 7.48 (s, I_{rel} = 3), 7.35 (s, I_{rel} = 1), 7.10 (s, fwhm = 24 Hz, I_{rel} = 1), 6.53 (s, fwhm = 26 Hz, I_{rel} = 2). IR (KBr, cm^{-1}): 3057 (w), 1597 (w), 1527 (m), 1512 (m), 1491 (s), 1441 (s), 1389 (s), 1360 (m), 1320 (w), 1300 (s), 1273 (m), 1221 (s), 1180 (s), 1163 (m), 1076 (m), 1005 (s), 978 (s), 964 (s), 878 (w), 818 (w). Anal. Calcd for $C_{88}H_{56}N_8ZrSb_2Cl_{12}$: C, 53.23; H, 2.84; N, 5.64. Found: C, 53.10; H, 2.58; N, 5.36.

Magnetic Susceptibility. Measurements on solid samples of **2** and **3** were performed on a Quantum Design MPMS SQUID magnetometer at 10 kG over the temperature range 6–300 K. Diamagnetic corrections based on Pascal's constants[14a] were applied (constitutive correction for TPP suggested by Eaton and Eaton[14b] was not included): -975×10^{-6} and -1189×10^{-6} cgsu mol^{-1} for **2** and **3**, respectively. The diamagnetism-corrected data for **3** were fitted to the following expression for the temperature-dependent susceptibility:

$$\chi = (Ng^2\mu_B{}^2/kT)[(2e^{2x}/(1 + 3e^{2x})] + \chi_{TIP} + p(Ng^2\mu_B{}^2/4kT)$$

where $x = J/kT$. The first term is the temperature-dependent susceptibility (Bleaney–Bowers equation)[15] derived from the general isotropic exchange Hamiltonian $H = -2JS_1 \cdot S_2$ for $S_1 = S_2 = {}^1/_2$, χ_{TIP} is the temperature-independent paramagnetism, and p is the mole percent of a paramagnetic impurity of $S = {}^1/_2$. Fitting parameters obtained from the least-squares procedure are $J = -870$ cm^{-1}, $g = 2.00$, $\chi_{TIP} = 1.1 \times 10^{-3}$ cgsu mol^{-1}, and $p = 0.063$.

X-ray Crystal Structure Determination. Crystals of **2** and **3** were grown by slow diffusion of either mesitylene (for **2**) or toluene (for **3**) into CH_2Cl_2 solutions of the compounds in sealed tubes under argon. Crystals were mounted in a sealed capillary tube with the mother liquor on an Enraf-Nonius CAD4 diffractometer using graphite-monochromated Mo Kα radiation. Crystals of **3** were marginally suitable for X-ray work. Unit cell parameters were determined by least-squares refinement of 25 reflections. Crystal data for **2** and **3** are summarized in Table I. Data collection was carried out at room temperature for **2** and at –100 °C for **3**. The intensities of three standard reflections, measured every 3 h of X-ray exposure, showed no systematic changes. All the calculations were carried out with the Enraf-Nonius MolEN package. The intensity data were corrected for Lorentz and polarization effects, and empirical absorption corrections (DIFABS) were also applied. The structures were solved by a combination of Patterson and difference Fourier methods and refined by full-matrix least-squares methods.

In the crystal structure of **2**, a CH_2Cl_2 molecule, the C atom of which takes a 4-fold symmetry position, was disordered and modeled by assuming that it takes four different orientations. Another CH_2Cl_2 molecule appeared to occupy a 2-fold symmetry site, but the C atom could not be located in the difference Fourier map. In the final model, all non-hydrogen atoms were refined anisotropically. The positions of hydrogen atoms (except for the solvate molecules) were calculated (C–H = 0.95 Å) and were included as fixed contributions to the structure factor. Each hydrogen atom was assigned an isotropic thermal parameter 1.2 times that of the atom to which it is attached. The final cycle of refinement on F, involving 1333 observations and 266 variables, converged to the agreement indices given in Table I.

Refinement of the structure of **3** proceeded smoothly, except for problems with severely disordered $SbCl_6^-$ ions and CH_2Cl_2 molecules. No thoroughly satisfactory model for the disordered species was found. However, the structure of the $[Zr(TPP)_2]^{2+}$ molecule did not seem to be significantly affected by the disorder. One $SbCl_6^-$ ion had two orientations in which the Sb atom occupied two sites (the occupancy factors were refined to be 0.61 and 0.39) and two Cl atoms (Cl1 and Cl2) occupied positions that were common to both sites. In the other $SbCl_6^-$ ion, Cl atoms were disordered spherically around the Sb atom; the small electron densities found at distances of 2.0–2.6 Å from the Sb atom were assigned Cl atoms (Cl11–Cl32) with fractional occupancy factors (0.1–0.6); the occupancy factors were assigned from the difference Fourier peak height and then adjusted so that the combined occupancy factors/thermal parameters had reasonable values. One CH_2Cl_2 molecule was well ordered. However, each of the two disordered CH_2Cl_2 molecules occupied two sites in which the molecule was disordered over two different orientations. In the final model, owing to the small number of data with $I > 3\sigma(I)$, only Zr and Sb atoms and Cl atoms whose occupancies were greater than 0.6 were refined anisotropically. The final cycle of refinement on F, involving 3196 observations and 699 variables, converged to the agreement indices given in Table I. Positional and equivalent isotropic thermal parameters for selected atoms of **2** and **3** are listed in Tables II and III, respectively.

Table I. Crystallographic Data for **2** and **3**

	2	**3**
formula	$C_{88}H_{56}N_8Cl_6SbZr \cdot 3CH_2Cl_2$	$C_{88}H_{56}N_8Cl_{12}Sb_2Zr \cdot 3CH_2Cl_2$
fw	1905.97	2240.44
space group	$P4/ncc$ (No. 130)	$P2_1/c$ (No. 14)
a, Å	21.260 (3)	18.555 (3)
b, Å	21.260 (3)	18.037 (2)
c, Å	18.042 (3)	27.468 (5)
β, deg		102.95 (2)
V, Å^3	8155 (2)	8959 (2)
Z	4	4
temp, °C	23	–100
d_{calc}, g cm^{-3}	1.551	1.661
radiation	graphite-monochromated Mo Kα (λ(Kα$_1$) = 0.709 26 Å)	
linear abs coeff, cm^{-1}	9.07	13.1
2θ limits, deg	$3 < 2\theta < 50$	$3 < 2\theta < 42.0$
no. of unique data with $I > 3\sigma(I)$	1333	3196
$R(F)$[a]	0.054	0.079
$R_w(F)$[b]	0.063	0.090

[a] $R = \sum||F_o| - |F_c||/\sum|F_o|$. [b] $R_w = [\sum w(|F_o| - |F_c|)^2/\sum w|F_o|^2]^{1/2}$; $w = 4F_o^2/\sigma^2(F_o^2)$; $\sigma(F_o^2) = [\sigma(I) + (pI)^2]^{1/2}$.

Table II. Positional and Equivalent Isotropic Thermal Parameters for Selected Atoms in **2**

atom	x	y	z	B_{eq},[a] Å^2
Zr	0.250	0.250	0.0821 (1)	1.64 (2)
N1	0.1565 (4)	0.2669 (3)	0.0130 (4)	2.0 (2)
N2	0.1765 (4)	0.1899 (3)	0.1504 (4)	2.1 (2)
C1	0.1283 (4)	0.3254 (5)	–0.0004 (6)	2.1 (2)
C2	0.0630 (5)	0.3163 (5)	–0.0181 (5)	2.6 (3)
C3	0.0515 (4)	0.2551 (6)	–0.0201 (5)	3.3 (2)
C4	0.1106 (5)	0.2229 (5)	–0.0015 (6)	2.2 (2)
C5	0.1175 (5)	0.1579 (5)	–0.0071 (6)	2.9 (2)
C6	0.1155 (5)	0.2058 (4)	0.1672 (6)	2.3 (2)
C7	0.0790 (5)	0.1508 (5)	0.1864 (6)	3.1 (3)
C8	0.1193 (4)	0.1005 (4)	0.1848 (6)	2.7 (2)
C9	0.1802 (4)	0.1250 (5)	0.1649 (6)	2.1 (2)
C10	0.2340 (4)	0.0900 (4)	0.1716 (5)	1.8 (2)

[a] $B_{eq} = (4/3)\sum_i\sum_j\beta_{ij}\mathbf{a}_i \cdot \mathbf{a}_j$.

(12) Adler, A. D.; Longo, F. R.; Finarelli, J. D.; Goldmatcher, J.; Assour, J.; Korsakoff, T. *J. Org. Chem.* **1967**, *32*, 476–477.
(13) Gans, P.; Marchon, J.-C.; Reed, C. A.; Regnard, J.-R. *Nouv. J. Chim.* **1981**, *5*, 203–204.
(14) (a) Boudreaux, E. A.; Muray, L. N. *Theory and Applications of Molecular Paramagnetism*; Wiley: New York, 1976. (b) Eaton, S. S.; Eaton, G. R. *Inorg. Chem.* **1990**, *19*, 1095–1096.
(15) Bleaney, B.; Bowers, K. D. *Proc. R. Soc. London* **1952**, *A214*, 451.

Table III. Positional and Isotropic Thermal Parameters for Selected Atoms in **3**

atom	*x*	*y*	*z*	B_{iso},[a] Å^2
Zr	0.7730 (1)	0.7469 (2)	0.06789 (9)	2.51 (5)
N1	0.8974 (9)	0.753 (1)	0.1096 (6)	1.8 (4)
N2	0.783 (1)	0.859 (1)	0.1119 (8)	2.4 (5)
N3	0.684 (1)	0.743 (1)	0.1168 (7)	2.8 (5)
N4	0.798 (1)	0.637 (1)	0.1154 (8)	2.7 (5)
N5	0.813 (1)	0.839 (1)	0.0196 (8)	2.4 (5)
N6	0.667 (1)	0.809 (1)	0.0237 (8)	2.5 (5)
N7	0.698 (1)	0.653 (1)	0.0246 (8)	2.4 (5)
N8	0.847 (1)	0.687 (1)	0.0224 (8)	2.1 (5)
C1	0.951 (1)	0.693 (1)	0.117 (1)	2.3 (6)
C2	1.024 (1)	0.717 (1)	0.1256 (9)	2.1 (6)
C3	1.017 (1)	0.791 (2)	0.128 (1)	2.7 (6)
C4	0.942 (1)	0.813 (2)	0.121 (1)	3.2 (7)
C5	0.917 (1)	0.888 (2)	0.124 (1)	2.6 (6)
C6	0.845 (1)	0.903 (2)	0.122 (1)	3.1 (6)
C7	0.829 (2)	0.980 (2)	0.140 (1)	5.1 (8)
C8	0.755 (2)	0.981 (2)	0.136 (1)	3.9 (7)
C9	0.731 (1)	0.903 (2)	0.125 (1)	2.7 (6)
C10	0.661 (2)	0.878 (2)	0.129 (1)	3.4 (7)
C11	0.641 (2)	0.803 (2)	0.126 (1)	3.4 (7)
C12	0.570 (1)	0.774 (2)	0.138 (1)	3.2 (7)
C13	0.583 (1)	0.702 (1)	0.1428 (9)	2.3 (6)
C14	0.645 (1)	0.682 (2)	0.126 (1)	2.6 (6)
C15	0.672 (1)	0.609 (2)	0.131 (1)	2.9 (6)
C16	0.743 (2)	0.590 (2)	0.126 (1)	3.5 (7)
C17	0.775 (2)	0.515 (2)	0.141 (1)	3.5 (7)
C18	0.843 (1)	0.521 (2)	0.136 (1)	2.7 (6)
C19	0.859 (1)	0.592 (2)	0.121 (1)	2.5 (6)
C20	0.930 (1)	0.619 (1)	0.1214 (9)	2.0 (6)
C21	0.883 (1)	0.844 (2)	0.010 (1)	2.5 (6)
C22	0.899 (1)	0.919 (2)	−0.004 (1)	5.2 (6)
C23	0.837 (2)	0.960 (2)	−0.004 (1)	3.1 (7)
C24	0.785 (2)	0.911 (2)	0.012 (1)	3.7 (7)
C25	0.709 (2)	0.933 (2)	0.008 (1)	5.1 (9)
C26	0.657 (1)	0.882 (1)	0.015 (1)	2.2 (6)
C27	0.579 (1)	0.904 (1)	0.0063 (9)	1.8 (5)
C28	0.541 (1)	0.840 (2)	0.008 (1)	2.7 (6)
C29	0.594 (1)	0.782 (1)	0.0182 (9)	1.5 (5)
C30	0.573 (1)	0.710 (1)	0.0153 (8)	1.3 (5)
C31	0.622 (1)	0.649 (1)	0.0163 (9)	1.6 (5)
C32	0.598 (2)	0.575 (2)	0.002 (1)	3.9 (7)
C33	0.656 (2)	0.534 (2)	−0.000 (1)	4.1 (8)
C34	0.718 (1)	0.581 (1)	0.0128 (9)	1.7 (5)
C35	0.790 (1)	0.563 (1)	0.0065 (9)	1.5 (5)
C36	0.849 (1)	0.613 (2)	0.010 (1)	2.9 (6)
C37	0.917 (1)	0.590 (1)	−0.003 (1)	2.2 (6)
C38	0.957 (1)	0.652 (2)	−0.0002 (9)	2.2 (6)
C39	0.914 (1)	0.712 (1)	0.0105 (9)	2.0 (6)
C40	0.930 (1)	0.784 (2)	0.004 (1)	3.1 (6)

[a] For Zr, which was refined anisotropically, the equivalent isotropic thermal parameter (B_{eq}; defined as in Table II) is given.

Results and Discussion

The dication $[Zr(TPP)_2]^{2+}$ was prepared by the chemical oxidation of $Zr(TPP)_2$ with 2.1 equiv of phenoxathiinylium hexachloroantimonate in CH_2Cl_2.[11] Crystallization from CH_2Cl_2/toluene yielded analytically pure **3** in 88% yield. The product is air-stable in the solid state but rather unstable in solution in air; it starts to decompose to the monocation complex $[Zr(TPP)_2]^+$ in CH_2Cl_2 solution in 30 min. The Soret band of **3** (372 nm) is shifted to higher energy compared to those of the neutral precursor **1** (396 nm) or of the monocation complex **2** (376 nm). While **2** is NMR silent, **3** in CD_2Cl_2 is not. Although the ^{1}H NMR signals of **3** are not clearly resolved even at −40 °C owing to the line broadening and overlap, the relative peak areas of four broadened signals (2:1:1:3) in the δ 6–8 ppm region indicate that these are due to the pyrrole and phenyl protons. The oxidized marker bands,[16] which support the π-cation-radical nature of metalloporphyrin complexes, appear at 1300 and 1273 cm^{-1} in the IR spectrum of **3**. The EPR spectrum of **3** in CH_2Cl_2 at 100 K exhibited only a weak signal at g = 2.009 (line width = 6.5 G) having no hyperfine structure that is very similar to that of the monocation **2**.[7a] Peak area of the EPR signal of **3** is only $\sim^1/_{10}$th of that of **2** when both spectra were obtained under the same conditions. No signal was observed at the half-field region. We therefore suspect that the signal may be due to a small amount of the monocation impurity.

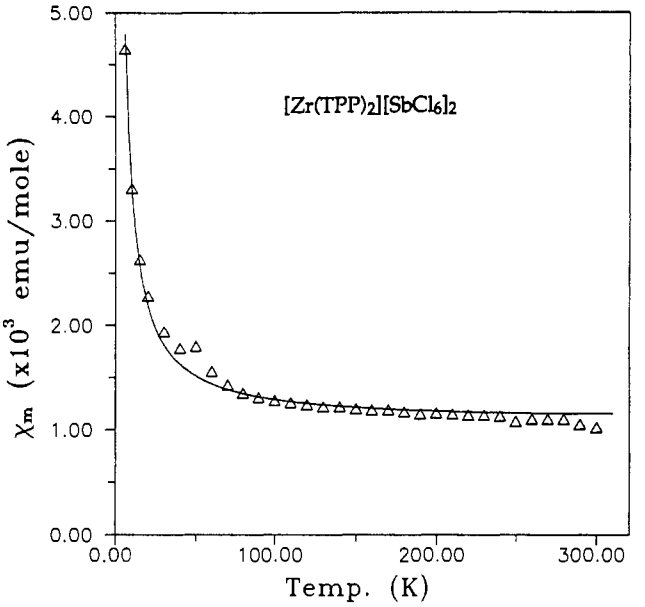

Figure 1. Plot of the molar magnetic susceptibility versus temperature for $[Zr(TPP)_2][SbCl_6]_2$. The solid curve represents the best fit (see text).

Magnetic Susceptibility. Magnetic susceptibilities of both **2** and **3** were measured over the temperature range 6–300 K. The diamagnetism-corrected data for the monocation **2** obeys the Curie law closely, and the effective magnetic moment is 1.7 μ_B. The diamagnetism-corrected data of **3** were fitted to the Bleany–Bowers equation[15] with the terms added for temperature-independent paramagnetism and for a paramagnetic impurity. The susceptibility data for **3** with the best fit are displayed in Figure 1. Fitting parameters obtained from the least-squares procedure are J = −870 cm^{-1}, χ_{TIP} = 1.1 × 10^{-3} cgsu mol^{-1}, and paramagnetic impurity = 6.3%. The large $-J$ values indicates that two unpaired electrons are strongly antiferromagnetically-coupled; the dication complex **3** therefore should be essentially diamagnetic. However, the origin of the large temperature-independent paramagnetism is uncertain. Similar observations have been reported in tightly coupled dimers. In $[Zn(OEP^{\bullet})(OH_2)]ClO_4$, which forms tight cofacial π–π dimers in the solid state, the unpaired electrons on the two porphyrin rings are so strongly coupled that the dimer is diamagnetic.[17] However, $[Ni(OEP)]_2(ClO_4)_2$, which has a similar cofacial structure, showed residual paramagnetism although this was ascribed to a decomposition product.[17] Taken together, these spectroscopic and magnetic susceptibility data suggest that the dication $[Zr(TPP)_2]^{2+}$ be formulated as a bis(porphyrin π-radical-cation) with a strong antiferromagnetic coupling between the unpaired electrons residing on the two porphyrin rings.

Near-IR Absorption. One of the characteristics of the π-radical-cation metal bis(porphyrin) complexes[2-5] is the presence of a broad band in the near-IR region. One notable feature of $[Zr(TPP)_2]^{2+}$ is that its near-IR band (780 nm; fwhm = 130 nm) is highly blue-shifted with respect to that of monocation $[Zr(TPP)_2]^+$ (1110 nm).[7,11] Similar large blue shifts of the near-IR bands of two-hole complexes with respect to those of the

(16) Shimomura, E. T.; Phillippi, M. A.; Goff, H. M.; Scholz, W. F.; Reed, C. A. *J. Am. Chem. Soc.* **1981**, *103*, 6778–6780.

(17) Song, H.; Orosz, R. D.; Reed, C. A.; Scheidt, W. R. *Inorg. Chem.* **1990**, *29*, 4274–4282.

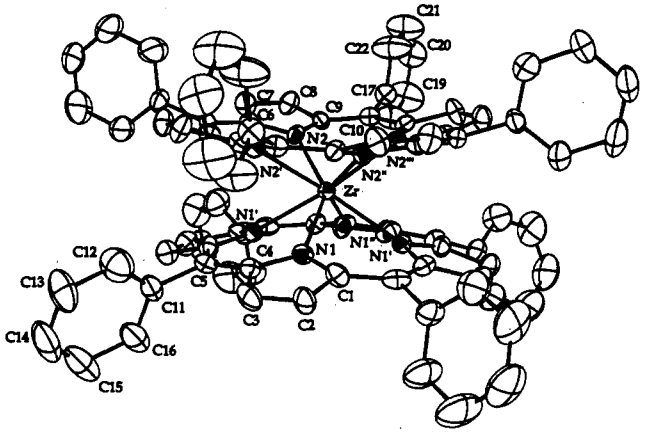

Figure 2. Structure of $[Zr(TPP)_2]^+$ in $[Zr(TPP)_2][SbCl_6]\cdot 3CH_2Cl_2$ (**2**) with atom labels.

corresponding single-hole complexes have been observed in lanthanide[2h,5f] and actinide[3] metal sandwich complexes: for example, $Th(TPP)_2^{2+}$ and a two-hole complex $Eu(TPP)_2^+$ exhibit the near-IR bands at 1080 and 1025[5f] (or 1030[2h]) nm, respectively; the corresponding single-hole complexes exhibit these bands at 1480 and 1330[5f] (or 1365[2h]) nm, respectively. Two interesting points should be made here. First, the much higher energies of the near-IR bands of the Zr complexes (both mono- and dications) than those of the other metal complexes are attributed to the smaller ionic radius of Zr^{4+}, which results in the stronger $\pi\pi$ interaction between the two porphyrin rings. A correlation between the energy of the near-IR band and the ionic radius of the central metal has been observed in the lanthanide metal sandwich complexes.[2d,h] Second, the large blue shift of the near-IR band of $[Zr(TPP)_2]^{2+}$ with respect to that of $[Zr(TPP)_2]^+$ is due to the stronger $\pi\pi$ interaction in the dication, as Bocian and co-workers[5f] pointed out for the absorption spectra of Eu(porphyrin)$_2^+$ vs Eu(porphyrin)$_2$ recently. According to the simple molecular orbital model[5] for sandwich complexes, the $\pi\pi$ interaction between the monomeric units splits the dimer MO's into bonding and antibonding. In the single-hole complexes, the bonding and antibonding dimer MO's are doubly and singly occupied, respectively; therefore, there is net bonding interaction due to $\pi\pi$ overlap. Removal of a second electron from the antibonding dimer MO increases the net $\pi\pi$ bond order. The enhanced $\pi\pi$ interaction in two-hole complexes relative to that in single-hole complexes results in blue shifts of the near-IR absorption bands which arise due to the transition of an electron from the bonding to the antibonding dimer MO. Since the enhanced $\pi\pi$ interaction must be manifested in the distance between the two porphyrin rings, we determined the X-ray structures of **2** and **3**. The latter is the first structurally characterized di(π-radical-cation) sandwich complex.

X-ray Structures of $[Zr(TPP)_2]^+$ and $[Zr(TPP)_2]^{2+}$. The structures of $[Zr(TPP)_2]^+$ in **2** and $[Zr(TPP)_2]^{2+}$ in **3** are shown in Figures 2 and 3, respectively. Selected bond distances and angles of these complexes are presented in Tables IV and V. $[Zr(TPP)_2]^+$ in **2** lies on a crystallographic 4-fold axis that passes through the zirconium atom and the centers of two porphyrin rings. Severely disordered counteranions and solvate molecules in the crystal of **3** resulted in somewhat large uncertainties in structural parameters. The coordination geometries around Zr in both mono- and dication complexes are similar to that of the neutral precursor.[7,18] Structural features of the three complexes are compared in Table VI. Most importantly, the average Zr–N bond distances shorten progressively as one proceeds from the neutral to the dication species (2.395 (6), 2.370 (7), and 2.35 (2) Å for **1**–**3**, respectively). The same is true for the interporphyrin distances: the separations of the $4N_p$ mean planes of the two porphyrin rings are 2.560, 2.480, and 2.43 Å, and the separations of the two 24-atom mean planes are 3.286, 3.188, and 3.12 Å for **1**–**3**, respectively. These structural features are consistent with the spectroscopic data described above and confirm that the $\pi\pi$ interaction between the two porphyrin rings in the dication is

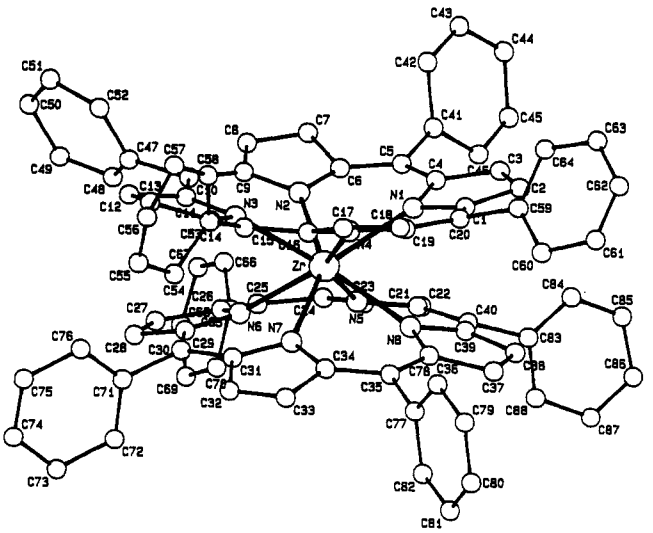

Figure 3. Structure of $[Zr(TPP)_2]^{2+}$ in $[Zr(TPP)_2][SbCl_6]_2\cdot 3CH_2Cl_2$ (**3**) with atom labels.

Table IV. Selected Bond Distances (Å) and Angles (deg) for **2**

Zr–N1	2.374 (7)	Zr–N2	2.366 (7)
N1–Zr–N1′ [a]	74.0 (2)	N1–Zr–N2″	73.8 (2)
N1–Zr–N1″	116.7 (3)	N1–Zr–N2‴	138.2 (2)
N1–Zr–N2	145.7 (2)	N2–Zr–N2′	74.2 (2)
N1–Zr–N2′	78.6 (2)	N2–Zr–N2″	117.2 (2)

[a] Primed, double-primed, and triple-primed atoms are related to the corresponding unprimed atom by a 4-fold symmetry.

Table V. Selected Bond Distances (Å) and Angles (deg) for **3**

Zr–N1	2.34 (2)	Zr–N5	2.35 (2)
Zr–N2	2.34 (2)	Zr–N6	2.35 (2)
Zr–N3	2.35 (2)	Zr–N7	2.34 (2)
Zr–N4	2.37 (2)	Zr–N8	2.32 (2)
N1–Zr–N2	75.7 (7)	N3–Zr–N5	134.0 (8)
N1–Zr–N3	117.6 (6)	N3–Zr–N6	72.5 (7)
N1–Zr–N4	73.6 (7)	N3–Zr–N7	81.5 (8)
N1–Zr–N5	81.1 (7)	N3–Zr–N8	150.2 (8)
N1–Zr–N6	148.2 (8)	N4–Zr–N5	149.4 (7)
N1–Zr–N7	133.7 (8)	N4–Zr–N6	136.4 (7)
N1–Zr–N8	69.3 (7)	N4–Zr–N7	72.1 (7)
N2–Zr–N3	73.6 (8)	N4–Zr–N8	80.7 (8)
N2–Zr–N4	117.3 (7)	N5–Zr–N6	72.5 (7)
N2–Zr–N5	71.3 (8)	N5–Zr–N7	117.0 (7)
N2–Zr–N6	79.3 (7)	N5–Zr–N8	74.3 (8)
N2–Zr–N7	148.9 (7)	N6–Zr–N7	75.6 (7)
N2–Zr–N8	133.8 (7)	N6–Zr–N8	118.1 (7)
N3–Zr–N4	74.5 (8)	N7–Zr–N8	75.3 (7)

Table VI. Comparison of Structural Features[a] of **1**–**3**[a]

	1	2	3
av Zr–N, Å	2.395 (6)	2.370 (7)	2.35 (2)
av Zr–Ct_N, Å	1.280	1.240	1.22
av Zr–Ct_P, Å	1.643	1.594	1.56
doming, Å	0.363	0.354	0.34
Ct_N–Ct_N, Å	2.560	2.480	2.43
Ct_p–Ct_p, Å	3.286	3.188	3.12
interporphyrin twist, deg	37	41	35

[a] Zr–Ct_N: Zr displacement from mean N plane. Zr–Ct_P: Zr displacement from mean 24-atom porphyrin plane. Doming = (Zr–Ct_P) – (Zr–Ct_N). Ct–Ct: interplanar spacing.

(18) The crystal structure of $Zr(TPP)_2$ in ref 7a was described incorrectly in space group $C2/c$ and should be in the orthorhombic space group $Fddd$. The revision did not affect appreciably the overall structure of the $Zr(TPP)_2$ molecule but improved the precision of the bond parameters: Kim, K.; Girolami, G. S.; Suslick, K. S. *Inorg. Chem.* **1992**, *31*, 716.

stronger than that in the monocation, which is in turn stronger than that in the neutral species.

The twist angles of the two porphyrin macrocycles in **2** and **3** are 41 and 35°, respectively, which are similar to that in **1** (37°). The porphyrin skeletons of **2** and **3** are severely domed, as indicated by the large separations between the $4N_p$ and 24-atom mean planes: 0.354 Å in **2** and 0.34 Å in **3**; the corresponding value for **1** is 0.363 Å. The doming is also illustrated by the deviations of atoms from the least-squares planes of the 24-atom porphyrin cores (Figures S1 and S2 in the supplementary material for **2** and **3**, respectively). The average deviation is 0.18 Å in both **2** and **3**, which may be compared to 0.21 Å in **1**. The individual pyrrole rings are essentially planar as usual; however, the dihedral angles between pyrrole rings and the mean porphyrin planes (listed in the supplementary material) are 14.7° in **2** and are in the range 13.0–17.3° in **3**. In contrast, two markedly different dihedral angles (23.9 and 9.9°) were found alternatively around the porphyrin ring in **1**. All these structural parameters related to deformation indicate that the deformations of the porphyrin cores in **2** and **3** are somewhat less severe than that in **1**. No unusual bond distances and angles for the porphyrin rings were found in **2** and **3**.

Conclusions

The di(π-radical-cation) complex $[Zr(TPP)_2][SbCl_6]_2$ has been synthesized and fully characterized. Spectroscopic and magnetic susceptibility data for the dication complex indicate a strong antiferromagnetic coupling between the unpaired electrons residing on two porphyrin rings. One notable feature of the dication complex is the high-energy near-IR absorption band. X-ray structures of $[Zr(TPP)_2][SbCl_6]$ and $[Zr(TPP)_2][SbCl_6]_2$ reveal that the interporphyrin distances shorten progressively as one proceeds from the neutral to the dication species. These structural features are consistent with the spectroscopic data and confirm that the $\pi\pi$ interaction between the two porphyrin rings is enhanced by oxidation. Further studies on the spectroscopic properties of the dication complex are underway.

Note Added in Proof. Buchler et al.[19] recently reported the spectroscopic and magnetic properties of $[Zr(OEP)_2](ClO_4)$ and $[Zr(OEP)_2](ClO_4)_2$ produced by the electrochemical oxidation of $Zr(OEP)_2$ (OEP = octaethylporphyrin dianion). Similar to our results on the TPP complexes, the monocation OEP complex is paramagnetic (μ_{eff} = 1.51 μ_B; temperature independent) while the dication complex is diamagnetic.

Acknowledgment. We thank Professor C. J. O'Connor for help in analyzing the magnetic susceptibility data of **3**. We gratefully acknowledge support from the Korea Science and Engineering Foundation and Dong-Il Scholarship Foundation. We also thank POSTECH for partial support of the X-ray analyses.

Supplementary Material Available: Tables of positional and isotropic thermal parameters, anisotropic thermal parameters, bond distances and angles, and dihedral angles between least-squares planes and diagrams showing displacements of atoms from the mean porphyrin planes for $[Zr(TPP)_2][SbCl_6]$ (**2**) and $[Zr(TPP)_2][SbCl_6]_2$ (**3**) (25 pages). Ordering information is given on any current masthead page.

(19) Buchler, J. W.; De Cian, A.; Elschner, S.; Fischer, J.; Hammerschmitt, P.; Weiss,R. *Chem. Ber.* **1992**, *125*, 107–115.